Electronic structure and microscopic model of $V_2GeO_4F_2$—a quantum spin system with $S = 1$

2007 J. Phys.: Condens. Matter 19 296206

(http://iopscience.iop.org/0953-8984/19/29/296206)

IOP PUBLISHING JOURNAL OF PHYSICS: CONDENSED MATTER

J. Phys.: Condens. Matter **19** (2007) 296206 (9pp) doi:10.1088/0953-8984/19/29/296206

Electronic structure and microscopic model of $V_2GeO_4F_2$—a quantum spin system with $S = 1$

Badiur Rahaman and T Saha-Dasgupta

S N Bose National Centre for Basic Sciences, JD Block, Sector 3, Salt Lake City, Kolkata 700098, India

E-mail: tanusri@bose.res.in

Received 15 March 2007, in final form 13 June 2007
Published 5 July 2007
Online at stacks.iop.org/JPhysCM/19/296206

Abstract

We present first-principles density functional calculations and downfolding studies of the electronic and magnetic properties of the oxide–fluoride quantum spin system $V_2GeO_4F_2$. We discuss explicitly the nature of the exchange paths and provide quantitative estimates of magnetic exchange couplings. A microscopic modelling based on analysis of the electronic structure of this systems puts it in the interesting class of weakly coupled alternating chain $S = 1$ systems. Based on the microscopic model, we make inferrences about its spin excitation spectra, which needs to be tested by rigorous experimental study.

(Some figures in this article are in colour only in the electronic version)

1. Introduction

Transition metal oxides provide a paradigm of unusual and novel phenomena. An interesting subset of this class of compounds are low-dimensional quantum spin systems (QSSs) [1]. Although these materials are structurally three dimensional, the effective interactions between the magnetic ions are highly anisotropic, reducing the dimensionality to one or quasi-one dimensional. The value of the spin associated with the magnetic ion is small, defining the quantum spins. Due to the quantum aspect, they often show a variety of interesting magnetic properties which are not present in their classical counterparts e.g. quantum spin systems having a gap in the spin excitation spectra form a category of compounds which are of special significance.

A very important issue in the study of low-dimensional QSS is the knowledge of the underlying spin model, given a specific compound. A possible route that is often used is to fit the measured susceptibility data with some assumed theoretical model. This method suffers from the drawback that the susceptibility data is quite insensitive to the details and two different models may be fitted to same data with two different sets of fitting parameters. $V_2P_2O_7$ [2] forms a classic example in this connection, which turned out to

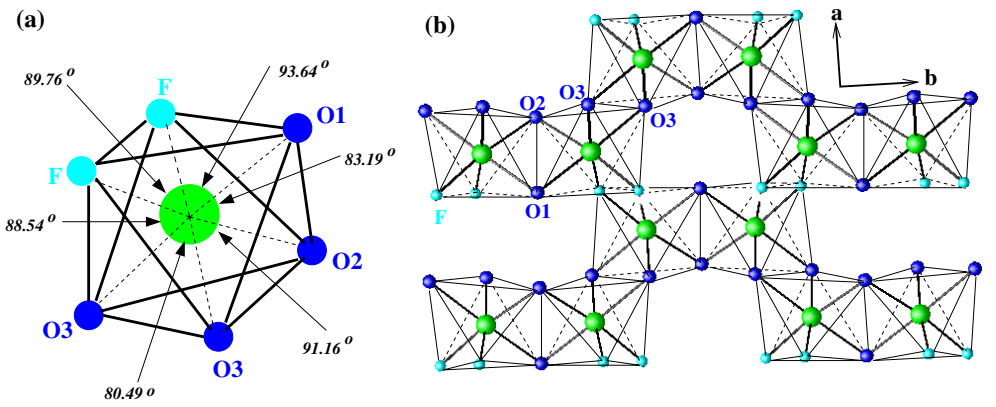

Figure 1. (a) The octahedral surrounding of V^{3+} ion consisting of four O-s and two F-s. Various bond angles are marked in the figure. The various bond lengths, in clockwise order starting from V–O1, are given by V–O1 = 1.990 Å, V–O2 = 1.998 Å, V–O3(1) = 1.996 Å, V–O3(2) = 2.014 Å, V–F(1) = 1.928 Å and V–F(2) = 1.864 Å. (b) Projection of zig-zag chains of VO_4F_2 octahedra.

be an alternating chain compound, while it was originally thought as an example of a spin-dimer. A microscopic investigation is therefore essential, particularly since the true nature of the underlying exchange network is often not what is expected from the crystal structure—one needs to take into consideration the chemical aspects too. Microscopic investigation also provides quantitative numbers corresponding to various exchange interactions. The muffin-tin orbital (MTO) based *N*th-order muffin-tin orbital (NMTO)-downfolding have been highly successful in arriving at an effective spin model, starting from the complex electronic structure of these materials. The methodology has been applied to a number of quantum spin systems like γ-LiV_2O_5, CsV_2O_5, $CaCuGe_2O_6$, $KCuCl_3$, $TlCuCl_3$, $TlCuCl_3$, $Cu_2Te_2O_5X_2$ (X = Br, Cl), TiOCl, and $Na_2V_3O_7$ [4]. The predicted microscopic models have been supported by subsequent experimental measurements [5], proving the usefulness of the methodology.

In this paper, we take up the case of a vanadium oxide fluoride system, namely $V_2GeO_4F_2$, which has recently been synthesized [6]. The nominal valence of the V ion in this compound is 3^+, which puts this system in the category of a $S = 1$ system. The preliminary susceptibility measurement indicates that the basic exchange interactions are of antiferromagnetic nature and have the signature of low-dimensional behaviour. The compound is therefore a promising candidate for a low-dimensional QSS. We present the local density approximation (LDA) electronic structure of the compound and, starting from such description, we derive a V-t_{2g}-only low-energy, few-orbital Hamiltonian by means of NMTO-downfolding calculations. We also present the quantitative estimates of the dominant exchange interactions and infer the possible spin-model based on those estimates.

2. Crystal structure

$V_2GeO_4F_2$ occurs in the primitive orthorhombic space group *Pnma* with four formula units in the unit cell and the lattice constants $a = 9.336$ Å, $b = 8.898$ Å and $c = 4.912$ Å [6]. The immediate surrounding of the V^{3+} ion constitutes two F^{2-} ions and four O^{2-} ions, giving rise to a distorted octahedral geometry with one short V–F, one intermediate V–F and four long V–O bonds (see figure 1(a)). The F atom belonging to the short V–F distance occupies the apical position of the octahedra, pointed approximately along the crystallographic *c*-axis,

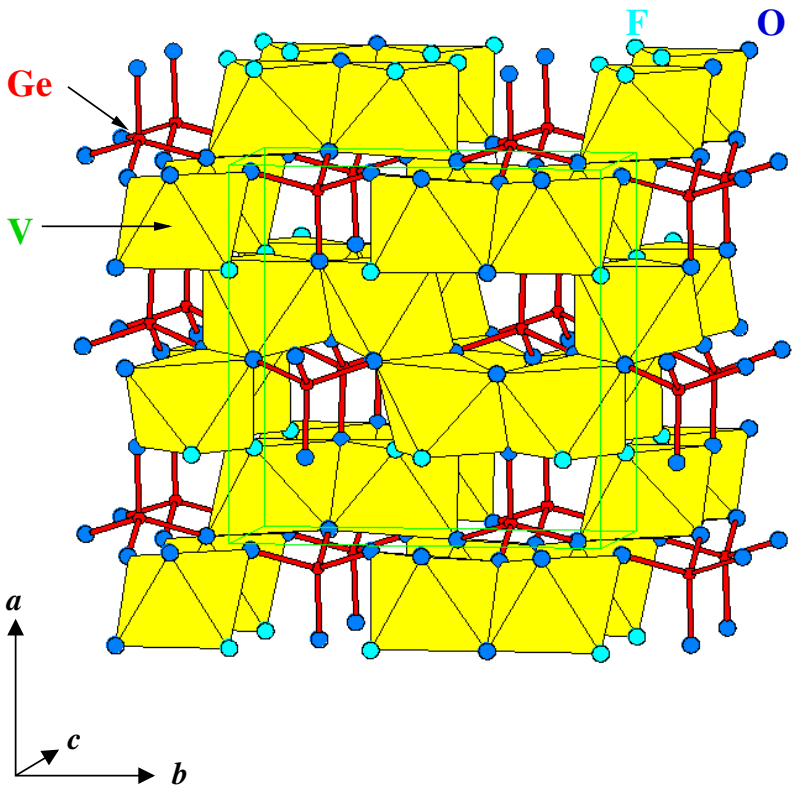

Figure 2. Crystal structure of $V_2GeO_4F_2$ showing the three-dimensional network of VO_4F_2 octahedra and GeO_4 tetrahedra.

while the other F belongs to the approximate *ab* plane. There are three different types of O atoms, O1, O2 and O3, as marked in figure 1. One of the O3 atoms occupies the second apical position and another goes in the plane. O1 and O2 occupies the other two positions in the plane. The nearest-neighbour (NN) VO_4F_2 octahedra edge-share via O1–O2 and form a pair, oriented along the crystallographic *b*-direction. The second-nearest-neighbour VO_4F_2 octahedra also edge-share via O3–O3, thereby giving rise to a zig-zag chain-like structure of VO_4F_2 octahedra of composition VO_4F_2, which is connected to the next zig-zag chain by means of corner-sharing via the plane F (see figure 1(b)). The Ge^{4+} ion is co-ordinated by four oxygen atoms, giving rise to GeO_4 tetrahedra which sit in the hollow formed between $V_2O_6F_4$ units. The co-ordination of GeO_4 tetrahedra with VO_4F_2 octahedra via the corner-shared O atoms gives rise to a three-dimensional network (see figure 2) with no direct connection between two VO_4F_2 octahedra along the crystallographic *c*-direction.

3. LDA electronic structure

The self-consistent electronic structure calculation within the framework of the local density approximation (LDA) of density functional theory (DFT) has been carried out in the tight-binding linear muffin-tin orbital (TB-LMTO) basis [7]. The basis set consisted of Ge sp, V spd, F sp and O sp. Eight different classes of empty spheres were used to space fill the system.

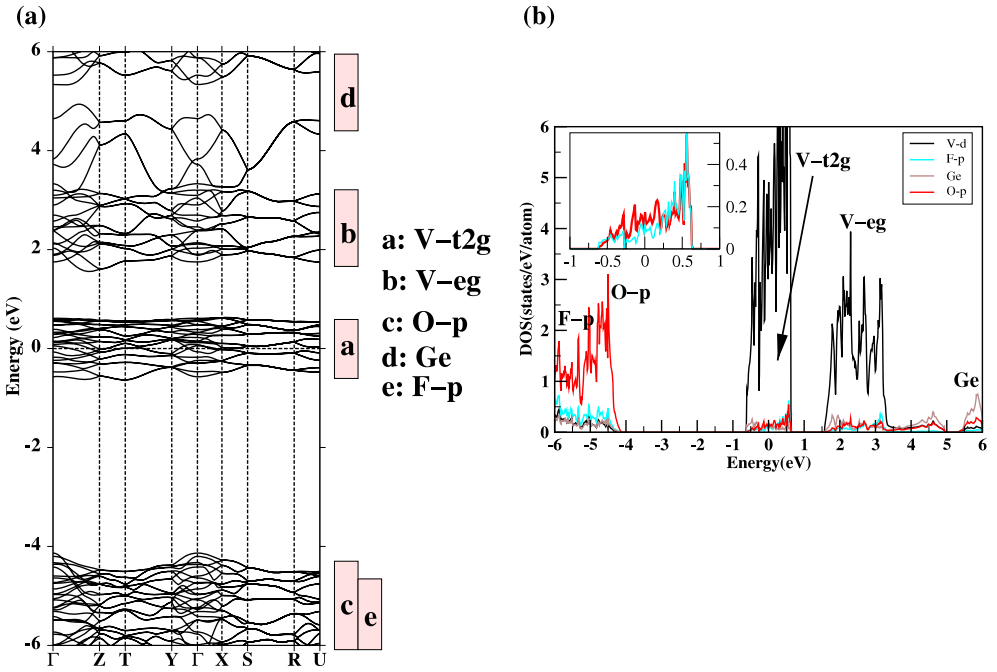

Figure 3. (a) LDA band structure of $V_2GeO_4F_2$. The bands are plotted along the high-symmetry points of the orthorhombic BZ, $\Gamma(0, 0, 0)$, $Z(0, 0, \pi/c)$, $T(0, \pi/b, \pi/c)$, $Y(0, \pi/b, 0)$, $X(\pi/a, 0, 0)$, $S(\pi/a, \pi/b, 0)$, $R(\pi/a, \pi/b, \pi/c)$ and $U(\pi/a, 0, \pi/c)$. The zero of energy is set at the LDA Fermi energy. The bars mark the energy regions with respective dominant orbital characters. (b) LDA site and orbital-projected density of states of $V_2GeO_4F_2$. The inset shows the F-p and O-p projected density of states in the region of dominant V t_{2g} character.

The self-consistency was achieved by using 64 k-points in the irreducible Brillouin zone (BZ). The calculated band structure and the corresponding density of states are shown in figure 3. The octahedral surrounding of anions around the V ion splits the V d-manifold into t_{2g} and e_g manifolds. The distortion of the octahedra further splits the strict degeneracy of t_{2g} and e_g manifolds with splitting of the order of $\approx$0.05 eV and a small admixture between t_{2g} and e_g states. This causes 24 V-t_{2g} bands to cross the Fermi level—there are eight V atoms in the unit cell, each contributing three t_{2g} bands. The V-e_g-dominated states lie higher up in energy, crystal split by about 1 eV from the V-t_{2g} bands crossing the LDA Fermi level. The O-p and F-p dominated bands are split from the V-d manifold by a gap of about 3.5 eV and occupy an energy range below -4 eV or so. The Ge-dominated states appear high up in energy and remain essentially empty. The dominant band characters spanning various energy ranges are shown by bars in figure 3(a). For V-d characters, the anion-based local co-ordinate is chosen with the local $\hat{z}$-axis pointing along the short V–F bond and the local $\hat{x}$-axis pointing approximately along the other V–F bond. Examining the density of states, we see that V-dominated states have contributions from both O-p and F-p. The O-p contribution is a bit larger than F-p, which indicates somewhat larger hybridization with O than with F (see the inset of figure 3(b)). This happens due to the larger on-site energy difference between V-d and F-p compared to that between V-d and O-p, although the V–O bonds are on average longer than the V–F bonds by about 0.1 Å.

We note that LDA predicts the system to be metallic. It is well known that LDA fails to describe the correct insulating ground state for strongly correlated electron system, as is the

case here. The inclusion of the missing correlation effect beyond LDA in a partially filled V-d manifold provides the insulating description of the system. We have checked this by treating the correlation within the LDA + U framework. Although LDA fails to provide the correct ground state for this class of materials, it describes the bonding and chemistry aspects correctly. This method has been highly successful in deriving the microscopic model based on such information [4] and the construction of Hubbard-like Hamiltonians by adding the missing correlation effect to the LDA-derived one-electron part. In spite of the failure of LDA in the prediction of the correct ground state, the computed one-electron part is found to be surprisingly robust and gives a very good account of the chemical aspect of even a correlated insulator, as is the case in discussion. Extraction of the essential LDA information, however, needs filtering of the full LDA details. In the following, we applied the Nth-order muffin-tin orbital (NMTO) based downfolding technique, which has been designed to serve this purpose.

4. NMTO-downfolding and the hopping interactions

In recent years, a muffin-tin orbital based NMTO-downfolding technique [3] has been proposed and implemented which goes beyond the scope of the standard TB-LMTO technique and succeeds in extracting the relevant information needed for the modelling of a complex crystalline solid from a full LDA calculation. This is done via an energy-selective procedure of downfolding which selectively picks up a few bands of interest out of the LDA all-band calculation by integrating out degrees of freedom that are not of interest, called passive channels, and retaining a few degrees of freedom, called active channels. The few-band, downfolded Hamiltonian is thus constructed in the basis of effective NMTOs which have the central character of an active orbital and tails shaped according to passive, downfolded orbital characters. For a well-converged isolated set of downfolded bands, these effective NMTOs span the same Hilbert space as the Wannier functions of the corresponding downfolded bands. The real-space representation of the downfolded Hamiltonian in the basis of downfolded NMTOs provide information on effective hoppings. For the present application, we generate the few-band, downfolded Hamiltonian constructed out of effective V-t_{2g} orbitals by integrating out all the degrees of freedom associated with Ge, O and F, and also the e_g states of V. This choice is driven by the fact that the vanadium is nominally in the V^{3+} state with two electrons in the t_{2g} manifold. Therefore these are the bands that appear close to the Fermi energy and contribute in defining the low-energy Hamiltonian. The downfolded band structure, in comparison with the full LDA band structure, is shown in figure 4. With a choice of two energy points of expansion, marked as E_0 and E_1 in the figure, the downfolded bands are indistinguishable from the full band structure within the region of interest. This indicates good convergence of the downfolded t_{2g} bands which, in the present case, form an isolated set of bands. The underlying NMTOs therefore *are* the corresponding Wannier functions.

In figure 5, we show the three t_{2g} Wannier functions which have the central xy, yz or xz character defined in the local co-ordinate system specified earlier, and have tails shaped according to integrated out O-p or F-p character. Shown are the orbital shapes with two different lobes, coloured differently. We note the pdπ antibonds formed between V-t_{2g} and O-p, and V-t_{2g} and F-p, with somewhat stronger weights at O sites compared to those at F sites, in conformity with the conclusions drawn from a density of states plot. We also note the non-negligible weight of the tails sitting at neighbouring V sites. The tails sitting at neighbouring V sites are shaped according to V-e_g-like symmetry that occurs due to the distorted geometry of VO_4F_2 octahedra and the resultant mixing between t_{2g} and e_g. The quantitative estimates of various hopping interactions, $t^{i,j}_{m,m'}$, between the orbital m at the V site, i, belonging to the central VO_4F_2

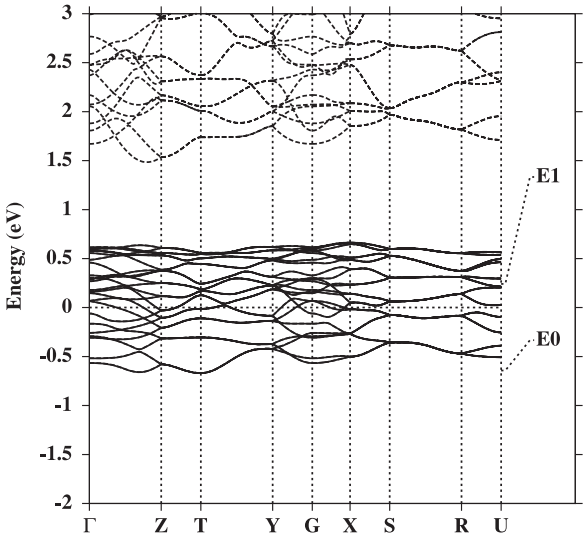

Figure 4. Downfolded t_{2g} (solid lines) bands of $V_2GeO_4F_2$ in comparison with LDA all-band structure (dotted lines). The zero of the energy is set at the LDA Fermi energy. E_0 and E_1 denote the energy points used in NMTO-downfolding calculations to pick up V-t_{2g}-only bands.

Table 1. Hopping interactions, $t^{i,j}_{m,m'}$ in meV between m and m' orbitals situated at V sites belonging to the central octahedra, marked as 0, and the neighbouring octahedra, marked as 1, 2 and 3 (see figure 5).

$(i, j) \rightarrow$ $(m', m) \downarrow$	Dimer intn (0–1)	Intn. via O (0–2)	Intn. via F (0–3)
xy, xy	296	−68	37
yz, yz	58	−177	16
xz, xz	−67	−79	−114
xy, yz	−56	−49	−125
yz, xy	56	49	1
xy, xz	−73	125	43
xz, xy	−73	125	15
yz, xz	−107	−23	16
xz, yz	107	23	−116

octahedra, and the orbital m' at the V sites js, belonging to neighbouring VO_4F_2 octahedra marked as 1, 2, 3 in figure 5 (m and m' run from 1 to 3, with $|1\rangle \equiv xy$, $|2\rangle \equiv yz$ and $|3\rangle \equiv xz$), are listed in table 1. We consider only the dominant V–V interactions, namely the nearest-neighbour (NN) V–V dimer interaction that proceeds via O1 and O2, the second-nearest-neighbour V–V interaction that proceed via two O3 atoms, and the third-nearest-neighbour V–V between two VO_4F_2 octahedra that corner share via the F atom. The rest of the interactions are an order of magnitude smaller. Examining the shapes of the downfolded xy, yz and xz Wannier functions, we conclude that the NN V–V interaction has to be strongest, contributing primarily via the V-xy–V-xy exchange path, while the 2NN V–V interaction contributes primarily via the V-yz–V-yz exchange path and the 3NN V–V interaction contributes primarily via V-xz–V-xz. The real-space representation of the downfolded Hamiltonian in the basis of Wannier functions, listed in table 1, also reveal strong contributions arising from inter-orbital hoppings between

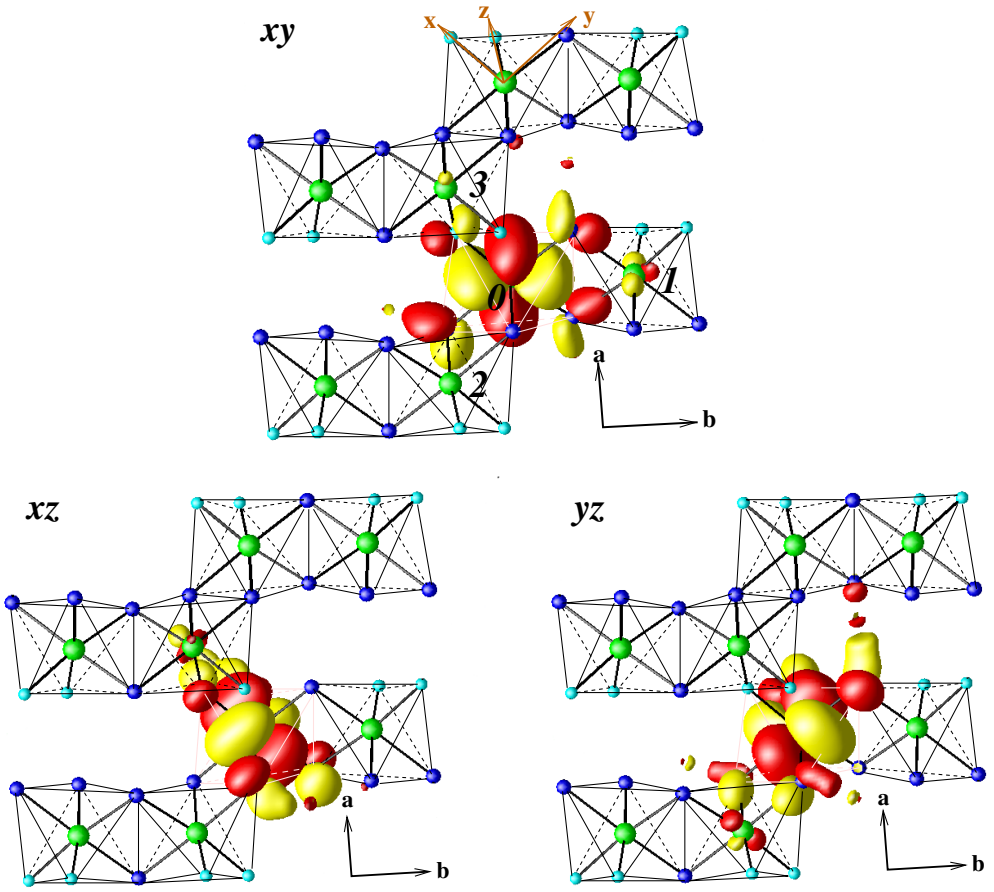

Figure 5. t_{2g} NMTOs for $V_2GeO_4F_2$. Shown are the orbital shapes, with the positive and negative lobes coloured red (dark grey) and yellow (light grey). The neighbouring octahedra surrounding the central octahedra (marked as 0) are numbered as follows: the NN octahedra edge sharing with the central octahedra via O1 and O2 are marked as 1, the 2NN octahedra edge sharing with the central octahedra via O3s are marked as 2, and the 3NN octahedra corner sharing with the central octahedra via F are marked as 3. The local co-ordinate system used to define the xy, xz and yz orbitals is shown in the first figure. The Ge atoms have been omitted from the structure for clarity.

V-yz and V-xz for NN, between V-xy and V-xz for 2NN, and between V-xy and V-yz, and V-xz and V-yz for 3NN.

5. Magnetic exchange interactions and the microscopic model

Starting from the t_{2g} Hubbard Hamiltonian given by $H^{\mathrm{LDA}}_{t_{2g},RR'} + U^{t_{2g}}_{R=R'}$, where U is the on-site Coulomb repulsion, one may derive the super-exchange (SE) Hamiltonian which, plugging in various hopping interactions, provides estimates of the magnetic interaction J^{ij} between V sites i and j. In deriving such an expression, we assume that the ground state is fully occupied by electrons in states $|1\rangle$ and $|2\rangle$, as confirmed by our LDA + U calculations. Following the standard approach of second-order perturbation, since the hopping interaction involves only two sites in the process of hopping, the difference between the excited state $|\beta\ \supset$ and the zeroth-order ground state $|\alpha\ \supset$ is only in these two sites. For both sites, the atomic $|\alpha\rangle$ is

Table 2. Magnetic exchange interaction, J^{ij}, between V^{3+} ions belonging to the central octahedra (marked as 0) and the neighbouring octahedra marked as 1, 2 and 3 (see figure 5).

i, j	J_{ij} (meV)
0–1 (dimer interaction)	38
0–2 (interaction via O)	13
0–3 (interaction via F)	5

a two-electron state, while one of the atomic $|\beta\rangle$ states is a one-electron state and the other is a three-electron state. The energy of the ground-state configuration is therefore given by $E_\alpha = 2(U_2 - J_H)$, where U_2 is the Coulomb repulsion between electrons belonging to different orbitals and J_H is the Hund's rule coupling. U, the Coulomb repulsion between electrons in the same orbital, is $U = U_2 + 2J_H$. On the other hand, the energy of the excited state E_β consists only of a three-electron site contribution, as the one-electron site does not contribute to the subspace of doubly occupied sites.

Considering the full, multiplet structure of excited states $|\beta_\lambda \supset$ with three-electron sites, it is possible to show that there are three distinct excited energies, $3(U_2 - J_H)$, $3U_2$ and $3U_2 + 2J_H$ [8]. Considering the various possible matrix elements between the ground-state configurations and excited states, and the energy differences between the Neél state and the ferromagnetic state, as done in [9] for the case of a t_{2g} manifold occupied by one electron, one gets

$$J_{SE}^{ij} = [(t_{11}^{ij})^2 + (t_{22}^{ij})^2 + (t_{12}^{ij})^2 + (t_{21}^{ij})^2]\left[\frac{1}{U + 2J_H} + \frac{1}{U}\right] + [(t_{13}^{ij})^2 + (t_{31}^{ij})^2 + (t_{23}^{ij})^2 + (t_{32}^{ij})^2]\left[-\frac{1/3}{U - 3J_H} + \frac{1/3}{U}\right].$$

In the above we have neglected the crystal field splitting, Δ, between different m and m' levels, which is about $0.012U$. Setting values of various $t_{mm'}^{ij}$ s and using $U = 4$ eV and $J_H = 0.8$ eV as appropriate for an early transition metal like V gives all the exchange interactions to be of antiferromagnetic nature (see table 2), in agreement with the preliminary susceptibility measurement [6]. The strongest interaction, J_1 (J_{ij}, $i = 0$, $j = 1$), is given by the nearest-neighbour pair, followed by the 2NN interaction, J_2, (J_{ij}, $i = 0$, $j = 2$), which connects two V ions via two O3 atoms and is about one-third of the strongest NN interaction. The 3NN interaction, J_3 (J_{ij}, $i = 0$, $j = 3$), that proceeds via the F atom is weak—1/8th of the NN V pair interaction. The above study therefore leads to a description of $V_2GeO_4F_2$ as that of a weakly coupled, $S = 1$ alternating chain compound with alternation parameter $\approx$0.3, where the alternation parameter is given by the ratio J_2/J_1.

Antiferromagnetic (AF) $S = 1$ spin chains give rise to rather interesting properties. For uniform chains, the ground state is an exotic quantum spin liquid with only short-range spin correlation and a gap in the excitation spectra, known as the Haldane gap [10]. Antiferromagnetic $S = 1$ chains that are not uniform, but instead feature alternating strong and weak bonds, are also gapped spin liquids, except at the quantum critical point [11]. However, for sufficiently strong alternation, as may possibly be the case in the present case, the so-called dimerized ground state is qualitatively distinct from the Haldane state. These differences are significant yet subtle [12]. In the literature, there has been considerable interest in the distinction of the behaviour of two such systems like $Ni(C_6D_{24}N_4)(NO_2)ClO_4$ (NTENP) and

$Ni(C_5H_{12}N_2)_2N_3(PF_6)$ (NDMAP) [13, 14]. It will be interesting to carry out similar studies to find out the nature of the possible gap in the case of $V_2GeO_4F_2$, which we predict to be a $S = 1$ quasi-one-dimensional bond-alternating AF.

6. Conclusion

In summary, using first-principles calculations, we have studied the electronic properties of the oxide–fluoride quantum spin system $V_2GeO_4F_2$, which has been synthesized recently. We have analysed the computed electronic structure in terms of NMTO-downfolding, which provided the effective hopping interactions between V^{3+} ions. Employing these estimates of hopping interaction, we derive the magnetic exchange interactions, which defines the system as a weakly coupled, antiferromagnetic $S = 1$ alternating spin chain. This forms an interesting class of QSS. Our prediction needs to be tested in terms of rigorous experimental study.

Acknowledgments

TSD would like to thank the Max-Planck-Gesellschaft (MPG)-India partner group program for the stay in Max-Plank-Institute (MPI) Stuttgart, Germany, where the problem was initiated, and the Swarnajayanti project for financial support. The authors gratefully acknowledge discussions with A Tyagi and R Valenti.

References

[1] See for a review Lemmens P, Gros C and Güntherodt G 2003 *Phys. Rep.* **375** 1
[2] Johnston D C *et al* 2000 *Phys. Rev.* B **61** 9558
[3] Andersen O K and Saha-Dasgupta T 2000 *Phys. Rev.* B **62** R16219 and references therein
[4] Valenti R, Saha-Dasgupta T, Alvarez J V, Pozgajcic K and Gros C 2001 *Phys. Rev. Lett.* **86** 5381
Valenti R and Saha-Dasgupta T 2002 *Phys. Rev.* B **65** 144445
Valenti R, Saha-Dasgupta T and Gros C 2002 *Phys. Rev.* B **66** 054426
Saha-Dasgupta T and Valenti R 2002 *Europhys. Lett.* **60** 309
Valenti R, Saha-Dasgupta T and Mila F 2003 *Phys. Rev.* B **68** 024411
Valenti R, Saha-Dasgupta T, Gros C and Rosner H 2003 *Phys. Rev.* B **67** 245110
Saha-Dasgupta T, Valenti R, Rosner H and Gros C 2004 *Europhys. Lett.* **67** 63
Saha-Dasgupta T, Valenti R, Capraro F and Gros C 2005 *Phys. Rev. Lett.* **95** 107201
[5] Zaharko O *et al* 2006 *Phys. Rev.* B **73** 064422
Johannsen N *et al* 2005 *Phys. Rev. Lett.* **95** 017205
[6] Achary S N, Tyagi A K and Köhler J 2002 *J. Solid State Chem.* **165** 74
[7] Andersen O K and Jepsen O 1984 *Phys. Rev. Lett.* **53** 2571
[8] Di Matteo S, Perkins N B and Natoli C R 2002 *Phys. Rev.* B **65** 054413
[9] Pavarini E, Yamasaki A, Nuss J and Andersen O K 2005 *New J. Phys.* **7** 188
[10] Haldane F D M 1983 *Phys. Lett.* A **93** 464
Haldane F D M 1983 *Phys. Rev. Lett.* **50** 1153
[11] Hagiwara M *et al* 1998 *Phys. Rev. Lett.* **80** 1312
[12] Hagiwara M *et al* 2005 *Preprint* cond-mat/0501207
[13] Escuer A *et al* 1997 *J. Chem. Soc. Dalton Trans.* 531
[14] Zheludev A *et al* 2003 *Phys. Rev.* B **68** 134438
Zheludev A *et al* 2004 *Phys. Rev.* B **69** 054414